Charge control and mobility in AlGaN/GaN transistors: Experimental and theoretical studies

Yifei Zhang
Applied Physics Program, The University of Michigan at Ann Arbor, Ann Arbor, Michigan 48109-1120

I. P. Smorchkova, C. R. Elsass, Stacia Keller, James P. Ibbetson, Steven Denbaars, and Umesh K. Mishra
Department of Electrical and Computer Engineering, University of California, Santa Barbara, California 93106

Jasprit Singh[a)]
Department of Electrical Engineering and Computer Science, The University of Michigan at Ann Arbor, Ann Arbor, Michigan 48109-2122

(Received 20 October 1999; accepted for publication 10 February 2000)

In this article we report on two dimensional sheet charge and mobility in GaN/AlGaN heterostructure field effect transistors. Both experimental and theoretical results are presented. Experimental results are reported on samples grown by metal organic chemical vapor deposition (MOCVD) and molecular beam epitaxy (MBE). Theoretical studies are done to examine how spontaneous polarization and piezoelectric effect control the sheet charge density. The studies also focus on how interface roughness, aluminum mole fraction in the barrier and phonon scattering influence mobility. We find that interface roughness is a dominant source of scattering in the samples reported. Due to the variation in growth techniques we find that the MBE samples have a smoother interface compared to the MOCVD samples. By carefully fitting the experimental data we present results on interface roughness parameters for MBE and MOCVD samples. © *2000 American Institute of Physics.* [S0021-8979(00)02010-7]

I. INTRODUCTION

Materials in the III–V nitride family (InN, GaN, and AlN) have physical properties that are very attractive for short wavelength light emission[1–4] and for high power/high temperature electronics.[5–9] Alloys and heterostructures based on these materials are therefore being studied with great interest. Recent advances in epitaxial growth control and processing have led to excellent transistor performance using the AlGaN/GaN heterostructure. High electron mobility transistors (HEMTs) have shown very good high power properties. It should be noted that in addition to providing semiconductors with large band gaps the nitrides have two very interesting features: (i) There is a spontaneous polarization present in the structures as a result of the cation and anion positions in the lattice.[10] In heterostructures the difference between spontaneous polarization of two layers can be used to create a high density of mobile carriers; (ii) In heterostructures with strain (resulting from epitaxy) the piezoelectric effects for the nitride system are so large that effective built-in fields of $\sim 10^6$ V/cm can be produced near the interfaces.[11] These two features have been exploited to design AlGaN/GaN HEMTs with very high sheet charge. It has been found[12] that in nominally undoped HEMT structures sheet charge densities greater than $10^{13}\,\mathrm{cm}^{-2}$ can be produced.

To fully exploit the potential of spontaneous polarization and piezoelectric effect in HEMTs and other electronic and optoelectronic devices, it is important that the parameters associated with these phenomenon be known accurately. In the AlGaN/GaN HEMT, for example, it is important to know the coefficients describing spontaneous polarization and piezoelectric effect. In addition it is important to know the values of band discontinuity and the Schottky barrier height. Finally it is important to know what issues control the mobility of electrons in the two dimensional electron gas (2DEG). In particular it is important to know what effect interface roughness has on transport since the heterostructure growth has not yet been perfected. At low temperatures interface roughness is expected to be an important source of scattering in undoped samples. Thus by examining the low temperature mobility in HEMT structures we can examine the role of interface roughness scattering in nitride heterostructures.

In this article we will present results on a series of experiments on charge control and mobility studies and use a theoretical formalism to fit the data. Experimental studies are based on samples grown by molecular beam epitaxy (MBE) and by metalorganic chemical vapor deposition (MOCVD). We will use the modeling to verify how accurate parameters given in the literature are and how important the role of interface quality is in AlGaN/GaN HEMTs. In Sec. II we will describe the experimental studies. In Sec. III we will provide details of the theoretical formalism used. In Sec. IV we will discuss the experimental results along with the theoretical fits. We will conclude in Sec. V.

[a)]Author to whom correspondence should be addressed.

II. EXPERIMENTAL STUDIES

The samples examined in this article are grown by MBE and by MOCVD. The two techniques would produce different quality of interfaces in general. Details of the MOCVD growth issues have been described in a previous article.[13] Heterostructures with 2–30 nm thick $Al_xGa_{1-x}N$ layers were grown by MOCVD on 3 mm thick semi-insulating GaN on *c*-plane sapphire substrates using the precursors trimethylgallium (TMGa), trimethylaluminum (TMA1), and ammonia. The growth of the GaN base layers was initiated on the sapphire substrate with an approximately 20 nm thick GaN layer grown at 525 °C, while the main GaN layer was grown at temperatures between 1040 and 1080 °C. A wide parameter range was explored for the growth of the AlGaN layers: the TMGa and the TMA1 flow were varied between 0.6 and 33 mmol/min and the ammonia flow between 0.08 and 0.32 mol/min. The growth temperature ranged from 800 to 1125 °C. The total gas flow and the reactor pressure were kept constant at 11 ℓ/min and 76 Torr, respectively. The properties of the 2DEG forming at the heterojunction were studied using $Al_xGa_{1-x}N$/GaN structures.

The MBE grown structures have been grown by rf plasma-assisted molecular beam epitaxy. The growth was performed in a Varian Gen II MBE system. Active nitrogen for growth was supplied by an EPI Unibulb nitrogen plasma source utilizing ultrahigh purity nitrogen (99.9995%) which was further purified by an inert gas purifier installed at the rf plasma source gas inlet. Elemental Ga (6 N) and Al (6 N) supplied from conventional effusion cells were used for the group III elements. Unintentionally doped GaN templates grown on (0001) sapphire by atmospheric pressure MOCVD were used for MBE growth of AlGaN/GaN structures. More details on the MBE growth procedure can be found in Ref. 14. The MBE grown films consisted of 0.25–0.3 μm thick GaN layers followed by $Al_xGa_{1-x}N$ regions of different thicknesses and alloy compositions. No intentional doping was performed during MBE growth. Double crystal x-ray rocking curve measurements (2θ–ω scans) were used to estimate the alloy composition in the top AlGaN layer. Both (0002) and (0004) reflections were studied. Assuming coherently strained AlGaN layers and utilizing the elastic constants given by Polian *et al.*,[15] the Al concentration was calculated from the GaN and AlGaN peak separation. The carrier concentration profiles in the AlGaN/GaN heterostructures were determined using capacitance–voltage measurements. The measurements were performed on the Schottky diode structures in which platinum was used for Schottky contacts while Ti/Al/Ni/Au layers were used to form the ohmic contact to unintentionally doped GaN. Temperature-dependent ($13\,K<T<300\,K$) Hall measurements were performed in Van der Pauw geometry on 1 cm×1 cm square samples. Indium was used to form the ohmic contacts to the structures under investigation.

III. THEORETICAL FORMALISM

In this section we will discuss the formalism used to understand the experimental observations. We will first give a brief discussion of spontaneous polarization and piezoelectric effect. Next we will discuss the charge control model. Finally we will discuss the mobility model.

A. Spontaneous polarization and piezoelectric effects

A number of material systems have spontaneous polarization effects arising from an imbalance of the cation and anion charges. Two of the most important material systems that have a large spontaneous polarization are the perovskites like barium titanate (spontaneous polarization 26×10^{-6} C/cm^2) and lithium niobate (spontaneous polarization 300×10^{-6} C/cm^2). In the nitride system the spontaneous polarization values are not as high but are significant enough to cause important effects in the band profiles of nitride heterostructures. The values of the spontaneous polarization[2] are

$$\text{GaN: } P_{sp} = -2.9\times10^{-6}\ \text{C/cm}^2,$$

$$\text{AlN: } P_{sp} = -8.1\times10^{-6}\ \text{C/cm}^2.$$

In addition to the spontaneous polarization, when a system is under strain, the relative positions of the cation and anion atoms in the unit cell can change. This can result in additional polarization effects in the system. In heterostructure growth, strain can be incorporated as a result of psueodomorphic growth of a thin overlayer on a substrate. In the nitride system, there are considerable differences in the lattice constants of the individual materials which can be exploited to tailor the strain values in a heterostructure. The lattice constant values *a* and *c* for GaN and AlN[16] are

$$\text{GaN: } a = 3.189\ \text{Å};\quad c = 5.185\ \text{Å},$$

$$\text{AlN: } a = 3.112\ \text{Å};\quad c = 4.982\ \text{Å}.$$

The two effects described above become important when heterostructures are grown. In the case of spontaneous polarization, the presence of a heterostructure between materials with different spontaneous polarization values causes a net charge at the interface, which causes built-in electric fields in the structure. Similarly, in the case where lattice constants of the components of the heterostructure are different, the resulting strain present (assuming minimal dislocation generation) causes charges at the interfaces due to the piezoelectric effect.

The magnitude and direction of the electric fields associated with spontaneous polarization and piezoelectric effect depend on the substrate, the growth orientation, and the nature of the surface (cation terminated or anion terminated). For the results given here we will discuss the most common growth conditions employed for the nitride systems where growth is on sapphire and is along the (0001) direction with the Ga terminated surface. The effective substrate (GaN in our studies) is defined by the thick overlayer that is grown on the starting substrate (sapphire). Once dislocations are generated, the thick overlayer assumes its relaxed lattice constant and acts as a substrate for the next layers as long as the growth is coherent, i.e., overlayer thickness is small enough to generate no dislocations. The overlayer now grows with a lattice structure that fits the in-plane lattice of the substrate

and has an out-of-plane lattice constant defined by total energy minimization. Thus a compressive strain in the plane of growth causes a tensile strain out of plane.

Consider for example a case where the effective substrate is GaN and an $Al_xGa_{1-x}N$ overlayer is grown coherently. The polarization is found to have the value[12]

$$P(x)=P_{pz}+P_{sp}=(-3.2x-1.9x^2)\times 10^{-6}\ \text{C/cm}^2 \\ -5.2\times 10^{-6}x\ \text{C/cm}^2. \quad (1)$$

We see that in this system the effects arising from piezoelectric effect and spontaneous polarization mismatch are comparable. Note that the two effects can have opposite directions as well, depending on the surface termination conditions and the lattice mismatch between the overlayer and the effective substrate. The electric field associated with the polarization given above is

$$F(x)=(-9.5x-2.1x^2)\ \text{MV/cm}. \quad (2)$$

We see that the built-in field and sheet charge values are very large. It is easy to produce fields around 10^6 V/cm and charge density around $10^{13}\,\text{cm}^{-2}$.

B. Charge control model

Our charge control model first obtains the potential profile in a HEMT structure by solving the Schrödinger equation and Poisson equation self consistently. The Schrödinger equation yields the confined charge terms in the Poisson equation which, in turn, determines the potential profile. This potential profile is fed back into the Schrödinger equation until the solution of the Poisson equation goes to convergence. The detailed formalism is described in Ref. 17.

C. Mobility model

Mobility is calculated by applying the Kubo–Greenwood (KG) formula.[17] The KG formula[18] for the conductivity of the electron under a small dc field is given by

$$\sigma_{DC}=\frac{2\pi e^2\hbar}{V}\sum_n\sum_m -\frac{\partial f}{\partial E}|\langle n|v|m\rangle|^2\delta(E_n-E_m), \quad (3)$$

where f is the Fermi–Dirac distribution function, v is the velocity operator, and V is the system volume. $|n\rangle$ is the electronic state under a certain potential configuration. The summation is over all the states close to the Fermi level. The number of electronic states involved in the summation depends on the temperature. Since a finite system is chosen for our numerical study, the delta function in the Kubo formula must be treated adequately. In a previous article,[17] we introduced an averaging process for the reduced momentum matrix. In this article, we use an alternative approach in which we replace the inner summation with integral and the delta function with Lorentzian function and Eq. (3) becomes

$$\sigma_{DC}=\frac{2\pi e^2\hbar^3}{m_e^{*2}}\sum_n\int\left(-\frac{\partial f}{\partial E_m}\right)N(E_m)|D_{n,m}|^2 \\ \times G_\Gamma(E_m-E_n)dE_m, \quad (4)$$

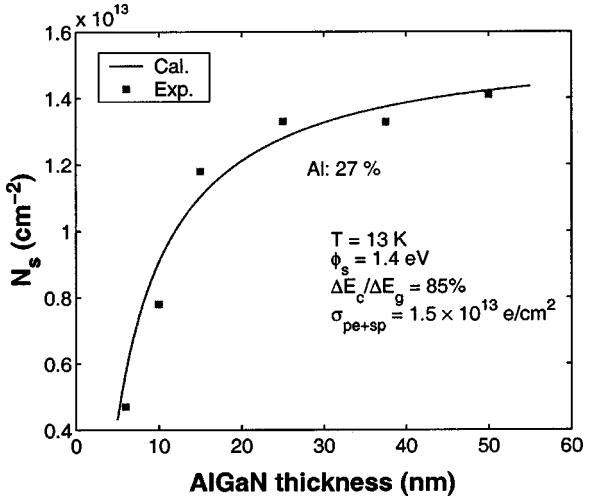

FIG. 1. Two dimensional sheet charge density as a function of AlGaN barrier thickness. The Al mole fraction in the barrier is 27%.

where m_e^* is the electron effective mass, $N(E_m)$ is the density of states function, $D_{n,m}$ is the reduced momentum matrix given by

$$D_{n,m}=\int \psi_n^*\frac{\partial\psi_m}{\partial x}d\mathbf{r},$$

and $G_\Gamma(E_m-E_n)$ is the Lorentzian function given by

$$G_\Gamma(E_m-E_n)=\frac{\Gamma}{\pi[(E_m-E_n)^2+\Gamma^2]}.$$

The parameter Γ in the conductivity expression represents scattering of electrons by inelastic processes such as phonons.[17] This is similar in spirit to the approach taken in deriving Mott variable range conductivity. This approach allows us to examine how phonon scattering and interface roughness scattering influence transport without treating them as independent scattering mechanisms.

We also examine mobility using the conventional approach based on Boltzmann transport theory. The interface roughness scattering rate in Born approximation is[18]

$$\frac{1}{\tau}=\frac{m^*e^2E_{avg}^2\Delta L_z^2L_{x,y}^2}{2\hbar^3}\int_0^{2\pi}E^{-k^2L_{x,y}^2\sin^2(\theta/2)}[1-\cos(\theta)]d\theta, \quad (5)$$

where E_{avg} is the average field given by $E_{avg}=\int E_z|\psi(z)|^2\,dz$.

IV. RESULTS

In the first set of results presented here we examine a series of samples in which the barrier layer is $Al_{0.27}Ga_{0.73}N$. The barrier thickness is altered from a high value of 50 to 6 nm. The measured sheet charge as a function of the barrier thickness is shown in Fig. 1 along with the calculated values. We find that we can get a good fit to the experiments with a set of parameters shown in the legend of Fig. 1. These parameters remain fixed for the other theoretical fits. Thus the polarization charge is simply scaled with Al composition for other results according to Eq. (1). The conduction band off-

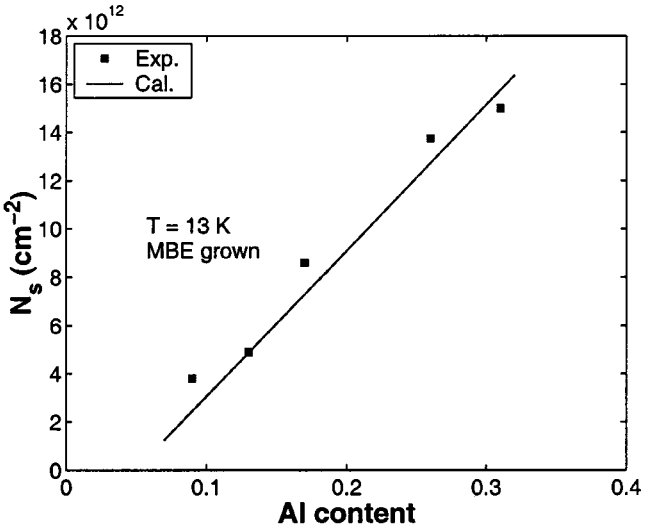

(a) MBE grown

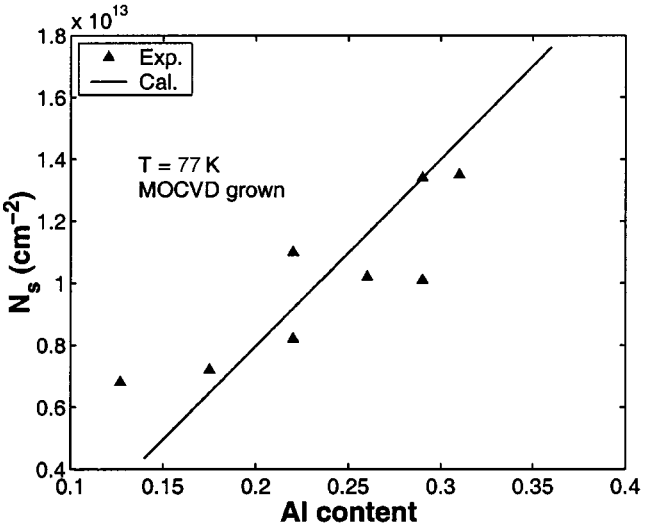

(b) MOCVD grown

FIG. 2. Sheet charge vs Al content in the barrier for: (a) MBE grown and (b) MOCVD grown samples. The solid lines are theoretical results using the charge control model presented and the parameters given in Fig. 1.

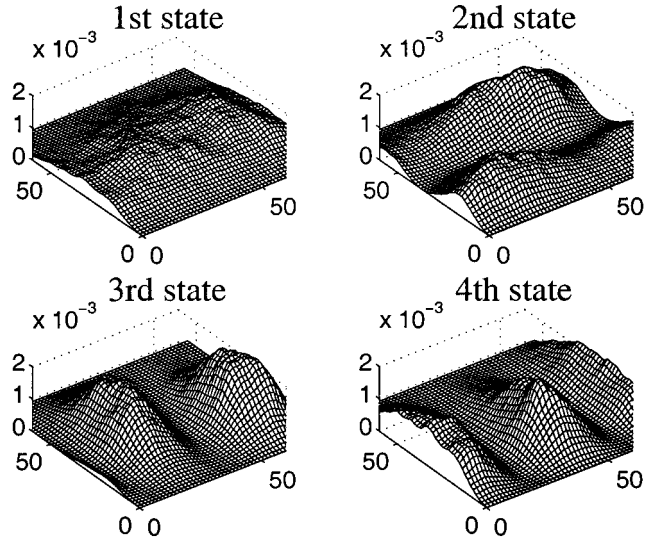

(a) Al: 9%

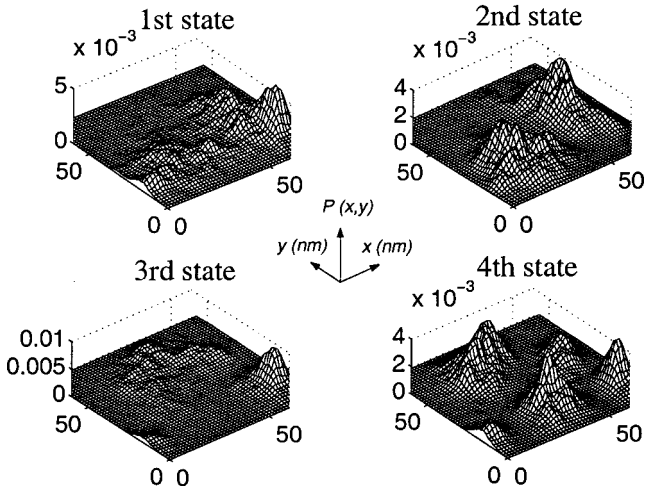

(b) Al: 20%

FIG. 3. Electronic states in the HEMT for an interface roughness described by a lateral extent of 15 Å and a height of 5 Å. (a) Results for a case where the barrier Al composition is 9%. (b) Results for a case where the barrier Al composition is 20%.

set is chosen to be 85% in this study. However, we find that the results are relatively unaffected by the value chosen.

Results of Fig. 1 show that the sheet charge is essentially unchanged as long as the barrier thickness is above 25 nm but drops rapidly as the thickness falls below this value. For barrier thickness below 5 nm the sheet charge is negligible. Of course the value of barrier thickness at which the charge in the 2D channel vanishes depends on the surface potential. In our study we find that the choice of surface potential (Schottky barrier) of 1.4 V gives the best fit to the experiments.

In Figs. 2(a) and 2(b) we show the results of sheet charge as a function of Al composition in the barrier for the MBE and MOCVD samples at temperatures 13 and 77 K, respectively. The barrier thickness for MBE and MOCVD samples is 31 and 20 nm, respectively. We find that there is a reasonable agreement between the theoretical model and the experiments. Discrepancies at lower Al content can be attributed to the fact that the barrier height remains constant. But this may not be correct because the surface barrier height may scale with the energy gap, i.e., get smaller at lower Al content.

To examine the effect of interface roughness on mobility at low temperatures we solve the problem as described in Sec. III in the presence of interface disorder. The interface is represented by a random placement of *A* and *B* type islands

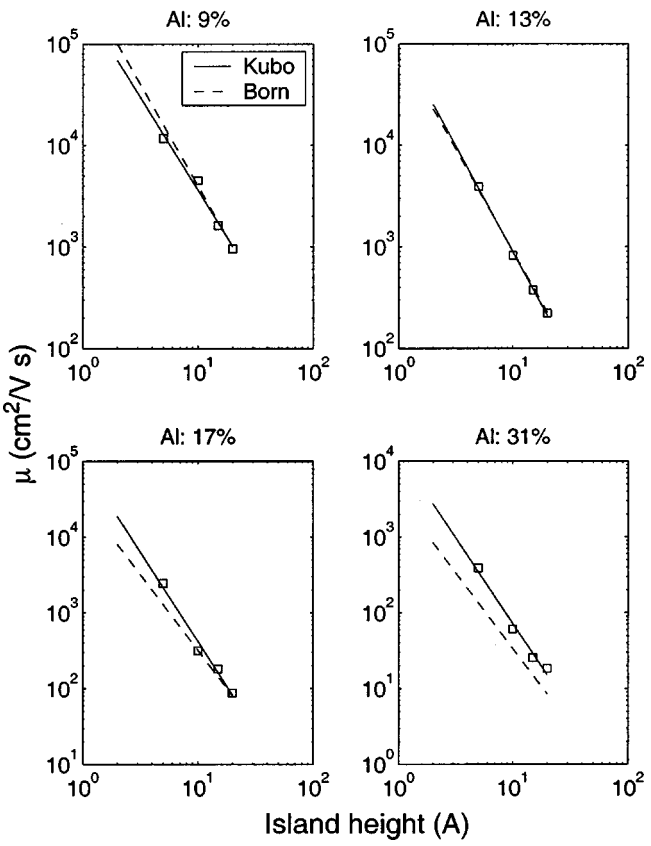

FIG. 4. Dependence of mobility in the channel on island height. Results are shown using Kubo formalism (calculated points are plotted along with a best fit) and Born approximation.

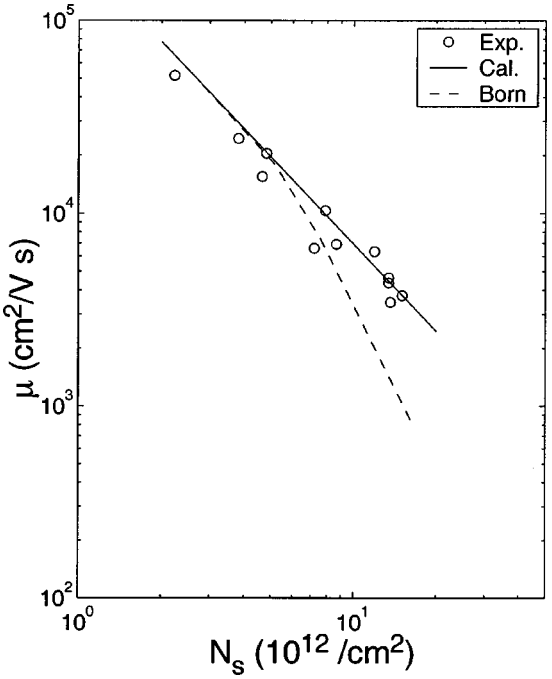

FIG. 5. Mobility vs sheet charge density. The experimental results are obtained from samples with varying Al mole fraction in the barrier region. The theoretical results use the same interface roughness parameters for all cases.

at the interface region. Here *A* represents the barrier region and *B* the GaN region. The lateral extent of the islands remains fixed at 15 Å in this study. This extent is suggested from TEM studies of the interface between AlGaN and GaN done in our laboratory. The island height is varied. A Monte Carlo approach is used to place islands randomly along the interface region. For mobility calculations the random sequence is varied and average results are reported. It should be noted that it is possible to find a different set of interface disorder parameters to fit the experimental results. For example, we can increase the lateral extent and decrease the island height to obtain the same mobility. As noted above our choice for the lateral extent has been based on TEM results on samples grown in our laboratory. The island height is then used as the adjustable parameter.

In Fig. 3 we show an interesting aspect of interface roughness. We show the calculated probability function for various electronic states in the plane of the interface. The interface region simulated in this study is 600 Å×600 Å. Figures 3(a) and 3(b) are for the sample with 9% and 20% Al composition, respectively. We see that for low Al composition sample, the low-lying electron states are coupled to the entire sample and only slightly vary from the wave functions for a perfect interface. This suggests at low Al content, the electron wave functions are extended and the interface roughness effect can be adequately treated by perturbation theory (Born approximation). However, at higher Al composition, we see that the low lying states are highly localized due to the very strong effect of interface disorder in the system. The Born approximation is no longer valid in dealing with the low lying states. Consequently, we use the KG formula to obtain the transport properties.

In Fig. 4 we show how the mobility values change as the island height changes from 5 to 20 Å for various Al compositions for MBE grown samples. The sheet charge value for each composition corresponds to the results shown in Fig. 2. We see that the relative effect of interface roughness scattering increases as the barrier Al composition increases as can be expected. Also shown in Fig. 4 are the mobility values obtained from the Born approximation. We see that at high barrier composition where localization effects are significant the Kubo formalism gives a higher mobility. This is because the formalism includes phonon assisted hopping effects that are not included in Born approximation. At low barrier compositions there is little difference between the two formalisms.

In Fig. 5 we present experimental and theoretical results on mobility versus sheet charge at low temperature. The experimental results shown are for MBE grown samples. It is important to clarify how the experimental results have been obtained. The experimental results are measured for each Al composition with specific sheet charge density. The theoretical results are calculated *assuming that the islands describing the interface roughness have the same parameters independent of the barrier composition*. Thus we assume that the interface quality is determined by GaN growth front and the barrier composition has no effect on the already grown GaN surface. Of course a higher barrier composition produces a larger potential fluctuation. Mobility versus sheet charge results using this model are shown in Fig. 5. We find that there

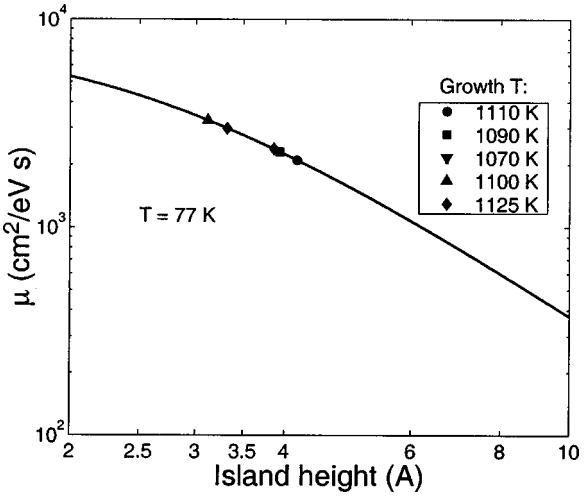

FIG. 6. Dependence of mobility on island height at 77 K and a sheet charge of $1.3\times10^{13}\,\mathrm{cm}^{-2}$. Also shown are data points obtained from MOCVD grown samples. The samples are grown at different temperatures.

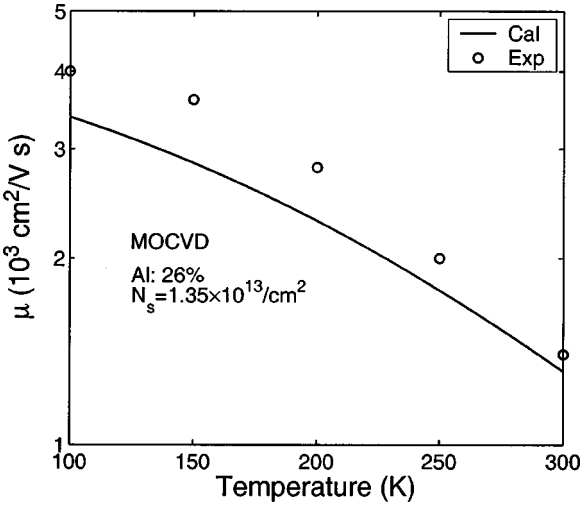

FIG. 8. Temperature dependence of mobility of MOCVD grown samples. Also shown are theoretical results. Results are for a sample with 26% Al in the barrier. The sheet charge in the channel is $1.3\times10^{13}\,\mathrm{cm}^{-2}$. The experimental results are Hall mobility while the calculations represent drift mobility.

is an excellent agreement over the entire range of the sheet charge values. The dashed curve represents the results by using Eq. (5). We see that the Born approximation results provide good agreement at low Al composition for the reason explained above.

In Fig. 6 we show experimental results for low temperature mobility measured in several MOCVD grown samples. The samples differ in the growth temperature used. It is expected that changes in growth temperature will alter the growth front and hence the interface quality. We also show a fit to the mobility using the interface island height as a variable. The theoretical result shows how sensitive mobility is to the interface roughness in the nitride system. We note that for the best mobility sample grown by MOCVD the interface island height we calculate is 3.0 Å. This is larger than the 2.5 Å island height we get for MBE grown samples.

In Fig. 7 we show theoretical results for mobility as a function of sheet charge. For this figure we use interface islands with a height of 3.0 Å and lateral extent of 15 Å. The sheet charge is varied by varying the gate bias in the structure. The study shows that mobility decreases as sheet charge increases. This is because the electron gas is squeezed closer to the interface and senses the disorder more. The variation of mobility with sheet charge has the same form as in Fig. 5 even though the sheet charge in Fig. 5 is altered because of the Al composition change in the barrier, while in Fig. 7 it is altered by applying a gate bias.

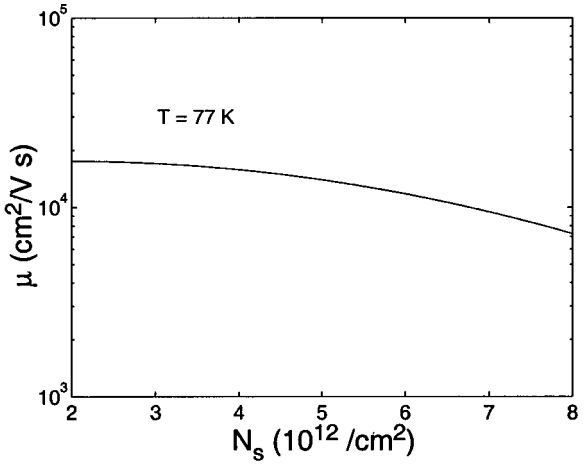

FIG. 7. Mobility as a function of sheet charge density for a fixed Al composition in the barrier. The sheet charge is altered through a gate bias.

Finally in Fig. 8 we show the temperature dependence of mobility in the MOCVD grown samples. Also presented is the theoretical fit to the data. To examine the temperature dependence we use a Monte Carlo approach to study how mobility changes at high temperatures. Both acoustic and optical phonons are included in the study. The diffusion coefficient is calculated by doing Monte Carlo simulations at zero electric field and the mobility is then obtained through Einstein's relation. The interface roughness effects are then included to obtain the total mobility. Results in Fig. 8 are for a sample with 26% Al in the barrier. The sheet charge in the channel is $1.3\times10^{13}\,\mathrm{cm}^{-2}$. The interface is described by islands of height 3.0 Å and a lateral extent of 15 Å. It is important to note that the experimental data shown is the Hall mobility and not the drift mobility. We see that if we use a Hall factor of 1.2 there is excellent quantitative fit between the experiments and the theoretical results.

V. CONCLUSIONS

In this article we have presented theoretical and experimental studies on charge control and mobility in GaN/AlGaN HEMTs grown by MBE and MOCVD. We find that the sheet charge density in the HFET channel is controlled by spontaneous polarization, piezoelectric effect, and barrier thickness. A careful fit to the data has allowed us to provide fairly accurate values for the Schottky barrier height and the coefficients controlling the polarization charges. We have also examined the dependence of the 2 DEG mobility on interface roughness, Al composition, and temperature. A fit

to the experimental data has allowed us to extract interface roughness parameters for both MBE and MOCVD grown samples. The MBE grown samples are found to have a very smooth interface. While the interface roughness description is not unique (i.e., it is possible to use other interface disorder models to fit the data), we see that interface disorder on the order of 1 monolayer or more reduces the mobility in the channel considerably. We also see that for low lying electronic states localization occurs in samples with high Al content in the barrier. This is because of the high carrier mass and the very high interface fields that arise.

ACKNOWLEDGMENTS

This work has been supported by Grant Nos. F001681 and F000629 from the US Office of Naval Research. The work at University of California, Santa Barbara was supported by the ONR IMPACT program.

[1] S. Nakamura, M. Senoh, N. Iwasa, S. Nagahama, T. Yamada, and T. Mukai, Jpn. J. Appl. Phys., Part 2 **34**, L1332 (1995); S. Nakamura, M. Senoh, S. Nagahama, N. Iwasa, T. Yamada, T. Matsushita, Y. Sugimoto, and H. Kiyoku, Appl. Phys. Lett. **69**, 3034 (1996).
[2] G. E. Bulman *et al.*, Electron. Lett. **33**, 1556 (1997).
[3] M. P. Mack, A. Abare, M. Aizcorbe, P. Kozodoy, S. Keller, U. K. Mishra, L. Coldren, and S. DenBaars, MRS Internet J. Nitride Semicond. Res. **2**, 41 (1997).
[4] A. Kuramata, K. Domen, R. Soejima, K. Horino, S. Kubota, and T. Tanahashi, Jpn. J. Appl. Phys., Part 2 **36**, L1130 (1997).
[5] O. Aktas, Z. F. Fan, A. Botchkarev, S. N. Mohammad, M. Roth, T. Jenkins, L. Kehias, and H. Morkoc, IEEE Electron Device Lett. **18**, 293 (1997).
[6] M. S. Shur and M. A. Kahn, MRS Bull. **22**, 44 (1997).
[7] Y. F. Wu, S. Keller, P. Kozodoy, B. P. Keller, P. Parikh, D. Kapolnek, S. P. DenBaars, and U. K. Mishra, IEEE Electron Device Lett. **18**, 290 (1997).
[8] U. K. Mishra, Y. F. Wu, B. P. Keller, S. Keller, and S. P. DenBaars, IEEE Trans. Microwave Theory Tech. **46**, 756 (1998).
[9] R. Dimitrov, L. Wittmer, H. P. Felsl, A. Mitchell, O. Ambacher, and M. Stutzmann, Phys. Status Solidi A **168**, R7 (1998).
[10] F. Bernardini, V. Fiorentini, and D. Vanderbilt, Phys. Rev. B **56**, R10024 (1997).
[11] W. Q. Chen and S. K. Hark, J. Appl. Phys. **77**, 5747 (1995).
[12] O. Ambacher *et al.*, J. Appl. Phys. **85**, 3222 (1999).
[13] C.-K. Sun, S. Keller, T.-L. Chiu, G. Wang, M. S. Minsky, J. E. Bowers, and S. P. DenBaars, IEEE J. Sel. Top. Quantum Electron. **3**, 731 (1997).
[14] I. P. Smorchkova *et al.*, J. Appl. Phys. **86**, 4520 (1999).
[15] A. Polian, M. Grimsditch, and I. Grzegory, J. Appl. Phys. **79**, 3343 (1996).
[16] *Properties of Group III Nitrides*, edited by, J. H. Edgar (INSPEC, London, 1994).
[17] Y. Zhang and J. Singh, J. Appl. Phys. **85**, 587 (1999).
[18] See for example, D. K. Ferry, *Semiconductors* (Macmillan, New York, 1991).